

# **VERIFICATION OF NWP TURBULENCE INTENSITY GUIDANCE USING EDDY DISSIPATION RATE FROM AIRCRAFT DATA**

Wai-Kin WONG\*, P.W. Chan and Alvin C.M. Li  
Hong Kong Observatory, Hong Kong, China

## **1. INTRODUCTION**

At the Hong Kong Observatory (HKO), the World Area Forecast System (WAFS) gridded forecast products from the two World Area Forecast Centres (WAFC) in London and Washington have been made available to airlines and pilot users since August 2008 for evaluation. The WAFS trial gridded forecast products including clear-air turbulence (CAT) potential, in-cloud turbulence, icing and cumulonimbus clouds (CB) are provided up to T+36h at a forecast interval of 6 hours, based on the Unified Model (UM) of the UK Met Office (WAFC London) and the Global Forecast System (GFS) of NOAA/NCEP (WAFC Washington) respectively.

This paper discusses the use of eddy dissipation rate (EDR) from commercial jets to verify the performance of NWP turbulence intensity products from the two WAFCs. Wind measurements recorded by flight data recorder are pre-processed by a band-pass filter algorithm to generate EDR. Contingency table approach is adopted to determine the hit, miss and false alarm of the clear air turbulence (CAT) potential from NWP models under different EDR thresholds. To assess the performance of model guidance, relative operating characteristic (ROC) curves are produced using different model CAT potential thresholds to determine the hit rate and false alarm. Additionally, the verification is applied to the turbulence intensity guidance from the Non-Hydrostatic Model (NHM), a new operational mesoscale NWP system in HKO. It is found that similar level of forecast skill on the moderate turbulence can also be obtained from NHM.

## **2. DESCRIPTIONS OF WAFS GRIDDED CAT PRODUCTS**

The WAFS gridded CAT forecast products are given as mean and maximum CAT potential with horizontal resolution of 1.25 degree in latitude / longitude. In vertical, the data are given

on isobaric levels from 400 hPa to 150 hPa at an interval of 50 hPa. Fig. 1 shows the maximum CAT potential forecasts (percentage depicted in color shade) from the two WAFCs at 06 UTC, 30 March 2010. While in general the overall patterns are quite similar, difference in the magnitude of maximum CAT potential can be seen, for example over the sub-tropical and mid-latitude region over Asia, Europe, Atlantic basin and the North America (circled areas in Fig. 1).

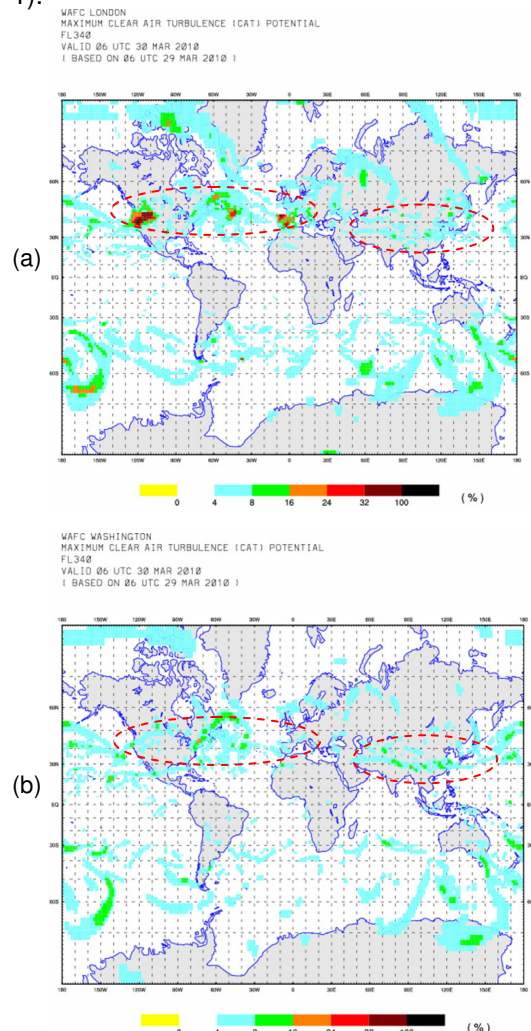


Fig. 1. Maximum CAT potential forecasts from (a) UK and (b) US WAFC on 250 hPa level (FL340) at 06 UTC 30 March 2010.

To facilitate the users' interpretation and assessment on performance of the gridded CAT potential, the verification of the CAT potential

\* Corresponding author address: Wai-Kin WONG, Hong Kong Observatory, 134A, Nathan Road, Kowloon, Hong Kong, China; email: [wk Wong@hko.gov.hk](mailto:wk Wong@hko.gov.hk).

may be made using well-defined quantities from aircraft data, e.g. derived equivalent vertical gust (DEVG) and eddy dissipation rate (EDR). To ensure such products to have sufficient quality for operational use, it is necessary to carry out their systematic verification over an extended period of time, covering different parts of the globe. It is noted that CAT potential from WAFCs is mostly verified using flight observations in North America and Europe (Gill et al 2010). In this paper, the performance of CAT potential is studied using EDR calculated from flight data in East and Southeast Asia.

### 3. FLIGHT DATA AND EDR

#### 3.1 Flight Data Distribution

About 1400 flights landed / departed from Hong Kong and flew over mainland China, East China Sea, South China Sea and Southeast Asia during Oct. 2008 – September 2009 are used in this study. Fig. 2 shows the geographical coverage of the flight paths.

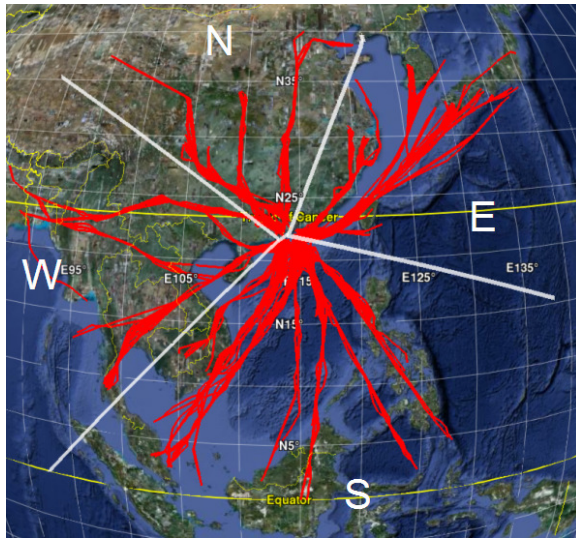


Fig. 2. Distribution of flight paths.

#### 3.2 Algorithm of Eddy Dissipation Rate (EDR)

Wind data from the flight data recorder (FDR) are processed to compute the eddy dissipation rate (EDR). In principle, EDR can be deduced by considering the power spectrum density of the measured vertical wind estimates  $S_w(\omega)$ :

$$EDR = \epsilon^{1/3} = \sqrt{\frac{1}{N} \sum_{i=1}^N \left[ \frac{S_w(\omega_i)}{0.7V^{2/3}(\omega_i)^{-5/3}} \right]}$$

where  $V$  is the airspeed and  $\omega$  is the angular frequency.

Using a wind-based algorithm, computation of EDR can be made alternatively by using a running mean standard deviation ( $\sigma_w$ ) calculation of the bandpass-filtered vertical wind. The inertial vertical wind component  $w$  is filtered with a digital band pass filter before  $\sigma_w$  is derived. Airspeed  $V$  is passed through a low-pass filter to obtain the average flying speed for the running time interval, and EDR is finally computed from filtered value of  $V$  and  $\sigma_w$  (Fig. 3).

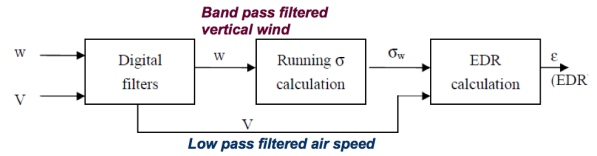


Fig. 3: A schematic diagram to calculate EDR from aircraft vertical wind ( $w$ ) and airspeed ( $V$ ).

### 4. VERIFICATION PROCEDURES

Two situations were considered for en-route aircraft:

- (i) mean  $EDR \geq 0.1 \text{ m}^{2/3}\text{s}^{-1}$ , representing light turbulence or above on average; and
- (ii) maximum  $EDR \geq 0.4 \text{ m}^{2/3}\text{s}^{-1}$ , corresponding to moderate turbulence level or above for the peak turbulence.

Based on the above maximum (mean) EDR threshold, the maximum (mean) EDR value of flight data along the flight path passing through the  $1.25 \times 1.25$  degree grid box is computed. For the WAFCs gridded maximum (mean) CAT potential forecasts, various thresholds from 0.1 to 40 are chosen to count the number of hits, misses, and false alarms in contingency table. Hit rate and false alarm rate are then calculated to plot the relative operating characteristic (ROC) curve. The total number of data points used in verification is about 19,000 and the distribution on various pressure levels are shown in Fig. 4.

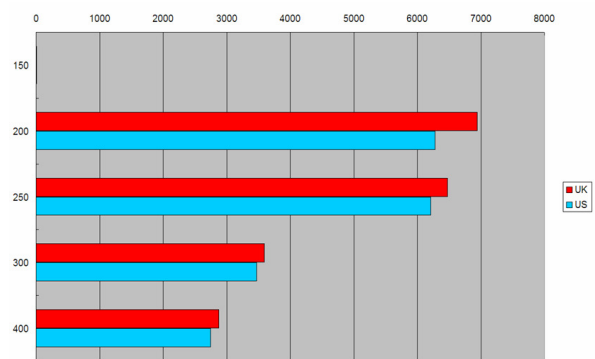


Fig. 4 Number of data points (x-axis) of gridded CAT potential on various pressure levels (in hPa) (y-axis) used in the verification (red: UK, blue: US).

## 5. RESULTS

### 5.1 Verification for different forecast hours

Fig. 5 shows the ROC curves for mean CAT potential products of WAFC London and WAFC Washington at forecast time of 6h (red), 12h (green), 18h (blue) and 24h (purple). For light turbulence or above on average, the two WAFCs have comparable skills, namely for a hit rate of 0.3–0.4, the false alarm rate is about 0.2.

In the case of moderate turbulence level or above for the peak turbulence (Fig. 6), the WAFC Washington has better skills (a false alarm rate of 0.2 with a hit rate of about 0.4 for T+12h and T+18h). However, the performance was much worse than that for high latitudes - which achieved a hit rate of about 0.9 for a false alarm rate of 0.2 for T+24 forecast when verified against the Global Aircraft Data Set (GADS data) for 50°N – 90°N (Albersheim *et al.* 2010). This suggests that development have to be carried out to improve the performance of CAT potential, especially in the tropical to subtropical regions.

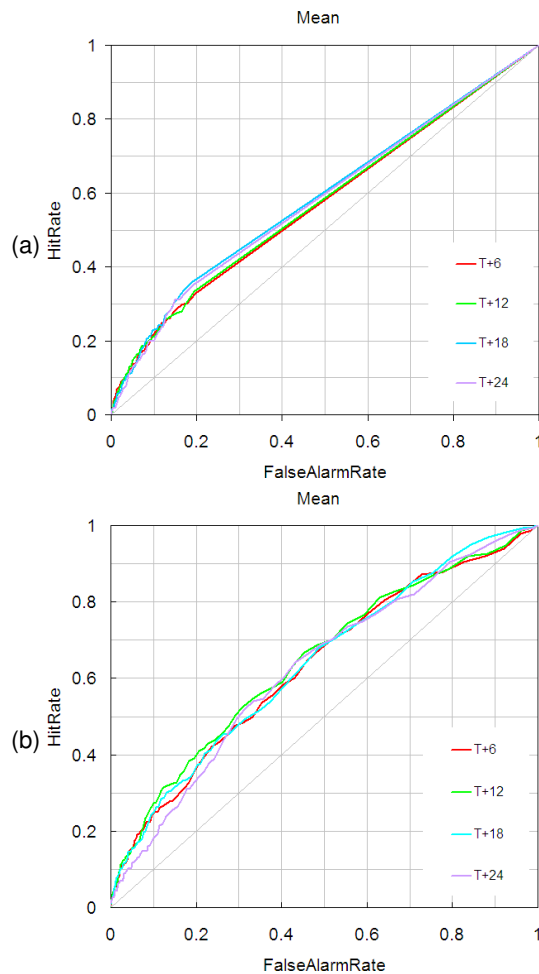


Fig. 5. ROC curves of mean  $EDR \geq 0.1 \text{ m}^{2/3}\text{s}^{-1}$  for (a) UK and (b) US CAT potential forecasts at T+6, 12, 18 and 24 hours.

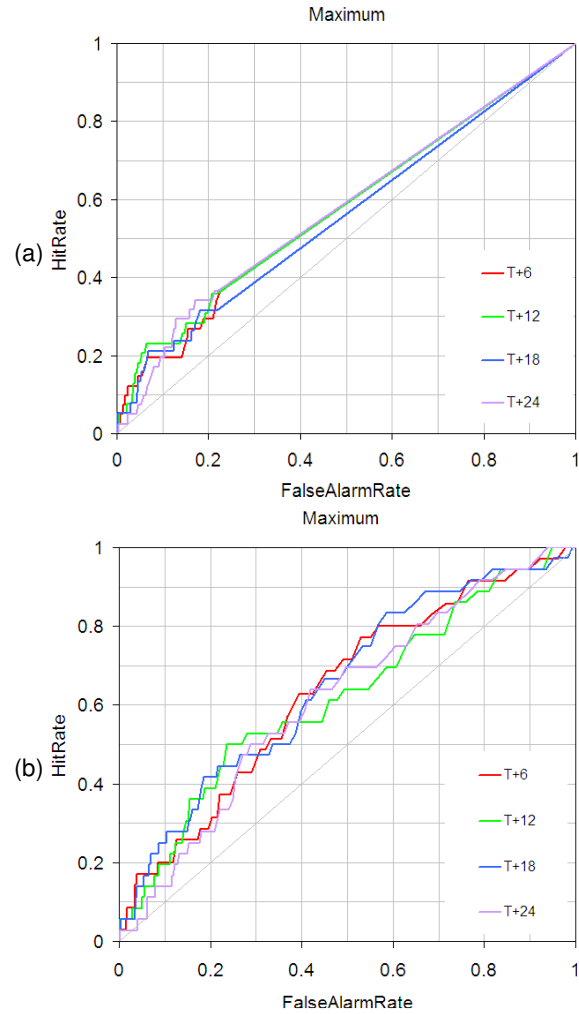


Fig. 6. ROC curves of maximum  $EDR \geq 0.4 \text{ m}^{2/3}\text{s}^{-1}$  for (a) UK and (b) US CAT potential forecasts at T+6, 12, 18 and 24 hours.

### 5.2 Verification for different flight areas

The datasets are further stratified into 4 quadrants (N/E/S/W) according to their flight paths (Fig. 2). Fig.7 and Fig.8 show the ROC curves using mean  $EDR \geq 0.1 \text{ m}^{2/3}\text{s}^{-1}$  and maximum  $EDR \geq 0.4 \text{ m}^{2/3}\text{s}^{-1}$  for T+24h forecast respectively. In the case for mean CAT potential from WAFC Washington, the performance over N, E and S quadrants are quite similar and attain a hit rate of 0.5 for a false alarm rate of 0.3. However, the forecasts over W quadrant have limited/no skill. It is noted that a larger geographical variation of performance of mean CAT potential is found in WAFC London product. Only ROC curves over E and N quadrants are above the diagonal and forecasts for flights over N quadrant reaching a hit rate of about 0.65 and a false alarm rate of 0.3. However, the forecasts over S and W quadrants in general have limited or no skill.

For the maximum CAT potential forecasts, the WAFC Washington CAT forecasts for E quadrant and the WAFC London CAT forecast for S quadrant have limited/no skill.

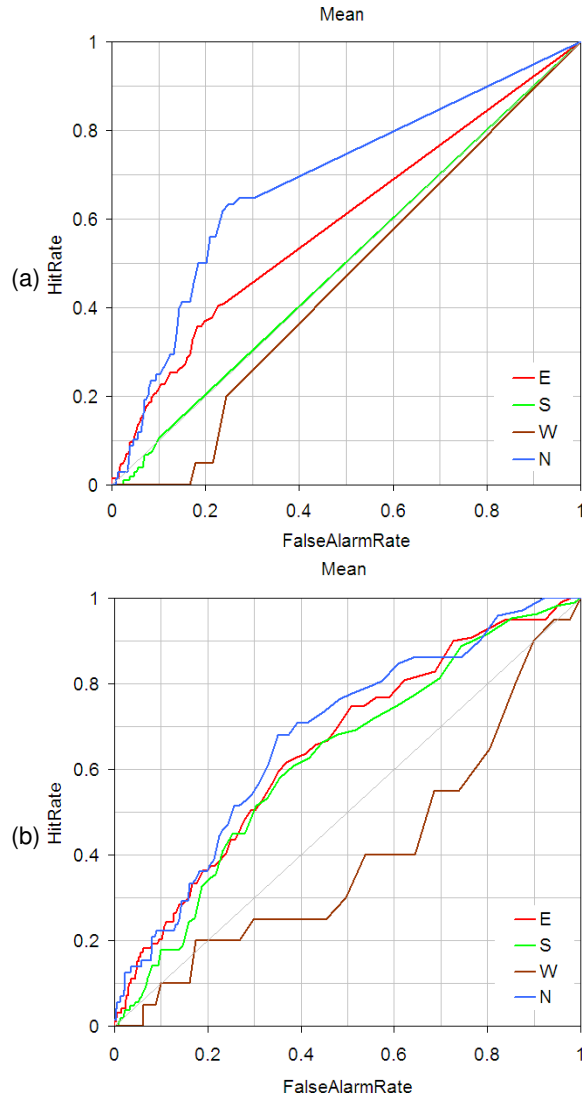


Fig. 7. ROC curves of mean  $EDR \geq 0.1 \text{ m}^{2/3} \text{ s}^{-1}$  for the T+24h of (a) UK and (b) US CAT potential forecasts over the four quadrants of flight routes.

It is noted that the present verification is based on data of one year only. While the percentage of data over the E and S quadrants are about 40% each, the percentage of data over the W and N quadrants were particularly sparse (only 6% and 12% of the total number of data points respectively) and only 3-4 turbulent events can be identified to verify the model forecasts.

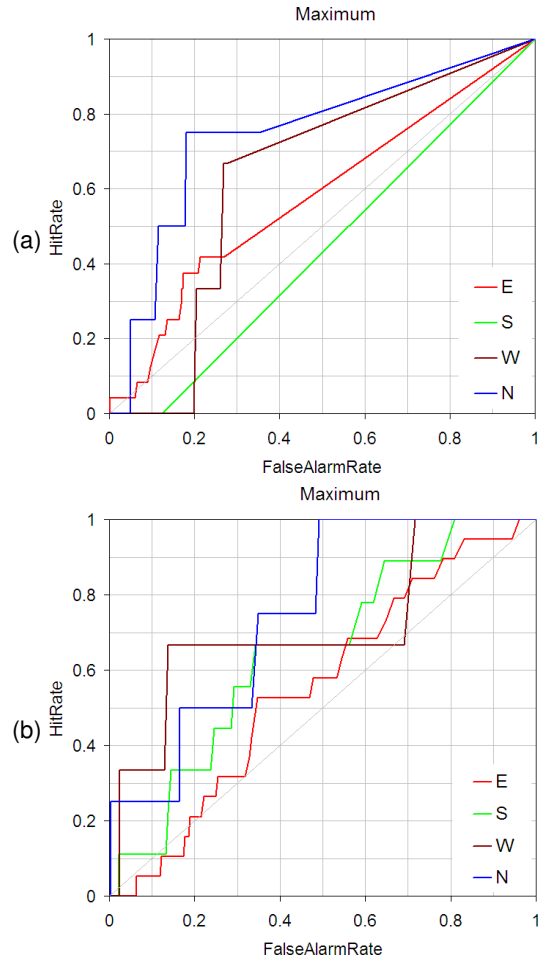


Fig. 8. ROC curves of maximum  $EDR \geq 0.4 \text{ m}^{2/3} \text{ s}^{-1}$  for the T+24h of (a) UK and (b) US CAT potential forecasts over the four quadrants of flight routes.

## 6. TURBULENCE INTENSITY GUIDANCE FROM NON-HYDROSTATIC MODEL

Turbulence intensity forecast guidance is under development for the Non-Hydrostatic Model (NHM), a new generation of operational NWP system at HKO (Wong et al 2011) to enhance the support in preparation of aviation significant weather chart and issuance of en-route turbulence warning. Turbulence index (TI) considering effects of vertical wind shear, horizontal wind deformation and convergence, and a modified version (DTI) including the tendency of horizontal divergence (Ellrod and Knox, 2010) are generated with horizontal resolution at  $0.1 \times 0.1$  degree in latitude/longitude and time interval of every 3 hours.

Fig. 9 shows an example of forecast TI map on 250 hPa level (FL340) for 18 UTC, 20 October 2010. Light to medium level of turbulence was forecast over eastern China to the East China Sea corresponding to the jet-stream areas ahead of a westerly trough, whereas medium to high turbulence intensity



was predicted over the South China Sea associated with upper tropospheric outflow region of the Severe Typhoon Megi.

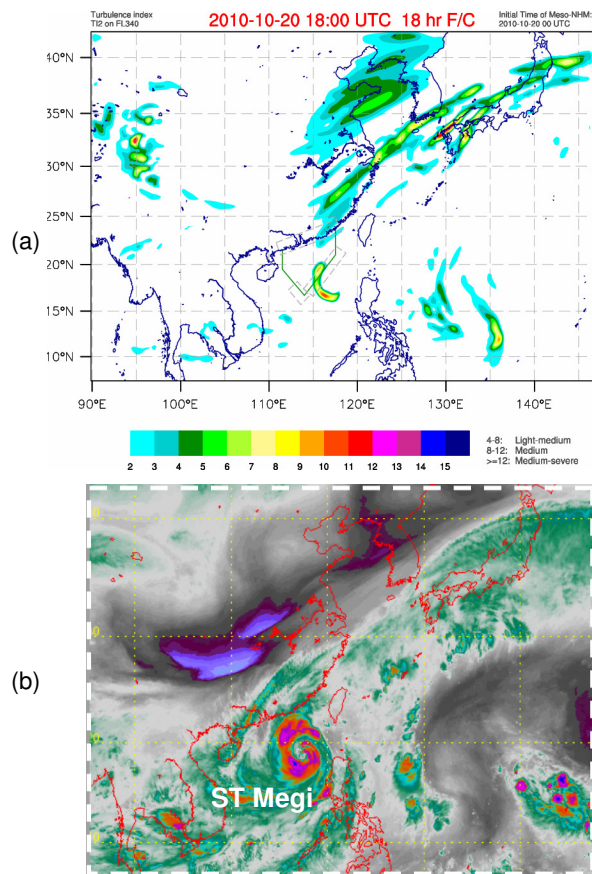


Fig. 9. (a) Forecast TI at 18 UTC 20 October 2010 from NHM; (b) enhanced water vapour imagery from MTSAT geostationary satellite.

Based on the model results and EDR from flight data during May-Aug 2009, TI and DTI attain a hit rate of about 0.5 for a false alarm of 0.35 for the 6-12 hours of forecast using a threshold of maximum EDR  $\geq 0.4 \text{ m}^{2/3} \text{ s}^{-1}$  (Fig.10). The performance is similar to forecasts from both WAFCs (Fig. 6).

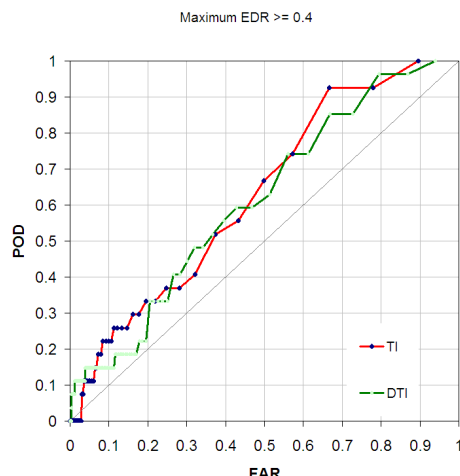


Fig. 10. Relative operating characteristics curves of TI and DTI forecasts from NHM.

To further improve the skill of NHM-based turbulence intensity forecast, other meteorological factors like the effects from the mountain waves, stability conditions and vertical motion associated with deep convections, will be considered to formulate a more robust guidance for en-route turbulence forecast.

## 7. SUMMARY

Verification of WAFS CAT potential products, using EDR data from commercial aircraft over Southeast Asia region, shows that the two global gridded turbulence forecasts have some difference in performance to capture the occurrence of en-route turbulence intensity. Further evaluation of the WAFS trial gridded forecasts using global data of more years will be needed in order to obtain more comprehensive verification results over different areas, to facilitate the use and interpretation of turbulence forecast products for different flight regions by pilots and aviation users.

The NHM-based turbulence intensity guidance shows promising skills to capture the medium level of turbulence. The verification will be continued to include more cases, as well as to investigate the performance of turbulence intensity guidance from NHM with more meteorological effects included.

## Reference

- Albersheim S., P.W. Chan, N. Gait, M. Graf, C. Hord, P. Josse, and L. Reid, 2010: Use of turbulence algorithms in the generation of SIGMET information. Third Meeting of ICAO Meteorological Warnings Study Group, Montreal, Canada, 15-18 November 2010.
- Ellrod, G. P., J. A. Knox, 2010: Improvements to an Operational Clear-Air Turbulence Diagnostic Index by Addition of a Divergence Trend Term. *Wea. Forecasting*, 25, 789–798.
- Gill, P., B. Lunnon, L. Reid, and A. Mirza, 2010: Objective verification of manual and automated forecasts of clear air turbulence from World Area Forecast Centres. 14th Conference on Aviation, Range, and Aerospace Meteorology, American Meteorological Society, Atlanta, Georgia, USA, 17-21 Jan 2010.
- Wong, W.K., P.W. Chan and C.K. Ng., 2011: Aviation Applications of a New Generation of Mesoscale Numerical Weather Prediction System of the Hong Kong Observatory. 24th Conference on Weather and Forecasting/20th Conference on Numerical Weather Prediction, American Meteorological Society, Seattle, USA, 24-27 Jan 2011.